High-Speed Prover Systems for Cost-Effective Mass Flow Meter and Controller Calibration

Speaker/Author: Harvey Padden
Bios International Corporation
10 Park Place
Butler, NJ 07405, U.S.A.
padh@biosint.com www.biosint.com
Phone: (973) 492-8400; FAX: (973) 492-8270

Abstract

There has long been a need for fast, cost-effective primary flow calibration systems to use with mass flow meters and mass flow controllers in the 1 sccm to 50 slm range. Exhibiting turndown ranges of hundreds to one, the provers described here use a clearance seal between a graphite piston and borosilicate glass cylinder. They are small, portable, fast, and contain no toxic materials. Reading cycle time is on the order of seconds.

Clearance-sealed volumetric Laboratory Master Provers were produced with an expanded uncertainty on the order of 0.07% (we will review the uncertainty analysis). Forming the basis of the system, they are dimensionally calibrated and primary. Stable flow generators were then applied as transfer flow sources in conjunction with the Laboratory Master Provers for the calibration of ML-500 production provers. Although we designed for 0.5% expanded uncertainty (at 2X), the analysis that follows shows results in the 0.35% to 0.4% range for most flows.

Fast enough for use at the point of manufacture, the ML-500 standardized provers form a primary calibration system for mass flow controllers. Used in conjunction with a stable flow generator, they are also very suitable for calibration of flow meters.

1. Introduction

There are a number of ways of measuring low gas flows. These include constant-displacement provers, laminar flow elements (LFEs) and constant-volume (rate-of-rise) instruments. Our ML-500 series of piston provers was designed for mass flow controller calibration and for other metrological applications requiring a combined expanded uncertainty of 0.5% or better.

We allocated 0.4% expanded uncertainty to the basic volumetric measurement and 0.3% for the temperature and pressure standardization. This would result in the required 0.5% when treated as a root-sum-square (RSS) value. We proceeded as follows:

- Develop master volumetric provers of 0.1 percent uncertainty to be used in calibrating the production ML-500s. Use an extended measurement path length, finer optical collimation and characterize the devices by direct dimensional (primary) means.

- Perform a detailed uncertainty analysis of the master volumetric provers. This is necessarily a major part of the ML-500 provers' analysis. As previously reported [1], the

master provers exhibited expanded uncertainties on the order of 0.07%. This prior work is summarized in sections 2 to 5.

- Characterize the reproducibility of the three sizes of ML-500 cells over their range of flows.
- Characterize the transfer uncertainty from the master cells to the target ML-500 cells.
- Analyze the uncertainties of the temperature and pressure standardization process.
- Characterize all other known error sources, such as drift.
- Calculate the expanded uncertainty.

2. Piston Prover Operating Principles and Variations

Constant-displacement systems are, perhaps, the simplest and most intuitive flow measurement devices. They have the extremely desirable characteristic of being characterized by the most basic of quantities: length and time. As flow is necessarily a derived unit, a dimensionally characterized system would be as close as possible to direct traceability from national dimensional standards.

An idealized piston prover would consist of a massless, frictionless, leak proof, shape-invariant and impermeable piston inserted within the flow stream and enclosed by a perfect cylinder (Figure 1). The time that the piston takes to move a known distance (which implies a known volume) then yields the volumetric flow as:

$$F = V / T = \pi r^2 h / T$$

Such a device would be as accurate as its physical dimensions and its clock, with almost insignificant drift mechanisms. Of course, such idealized devices do not exist. Historically, three basic practical versions of piston provers have been employed.

2.1. Bubble Devices

In their most basic form, piston provers can be nothing more than a calibrated burette within which a soap-film bubble rises with the gas flow. A stopwatch can be used to time the bubble's passage through a known volume between two marks. More modern bubble calibrators use optical bubble detection and an internal computer. The accuracy of any practical bubble device is limited by:

- Vapor pressure of water
- Shape variation of the bubble
- Permeability of the bubble
- Fluid viscosity changes with evaporation
- Variation of cylinder working diameter from dried and prior-reading bubble solution

The above-described uncertainties limit the usefulness of bubble devices. Vapor pressure alone can account for ±1.5% uncertainty. Bubble devices are of value when the insertion pressure must be as constant as possible, such as measurement of a very highly unregulated source.

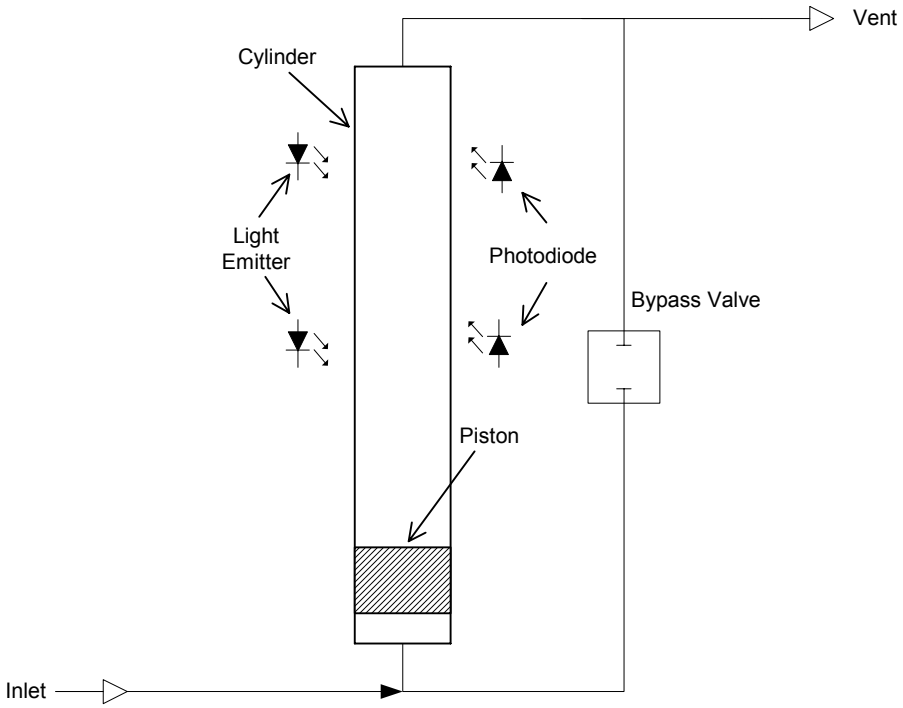

Figure 1. Idealized Automatic Piston Prover

2.2. Mercury-Sealed Provers

Mercury-sealed provers remedy some of the shortcomings of bubble calibrators. A rigid piston has the advantage of shape-invariability and impermeability, while gaining the disadvantages of requiring a seal and having a more significant piston mass.

In a laboratory calibrator used with high-stability flow sources, the piston mass can be made to cause minimal uncertainty. However, there is still the problem of sealing the piston. The best solution to date had been the use of a mercury piston ring to fill the gap between the piston and the cylinder. Its friction is very low and its vapor pressure is acceptable. However, piston speeds must be kept low to avoid loss of the mercury seal, limiting maximum flow rates and increasing measurement cycle time. A mercury seal also has the disadvantage of toxicity.

2.3. Clearance-Sealed Provers

The DryCal clearance-sealed prover uses a piston and cylinder fitted so closely that the viscosity of the gas under test results in a leakage small enough to be insignificant. For reasonable leakage rates, such a gap must be on the order of 10 microns. As a practical matter, the piston and cylinder are made of graphite and borosilicate glass because of their low, matched temperature coefficients of expansion and low friction[1].

Such a device comes close to the ideal. The piston is shape invariant, impermeable and virtually frictionless. There is no vapor pressure from a bubble or sealant. The instrument can utilize high piston speeds, resulting in a measurement repetition rate rapid enough to be considered quasi-continuous.

An uncertainty analysis for such an instrument has unique considerations. The static uncertainties must be evaluated in a manner similar to that used for mercury-sealed provers. In addition, though, dynamic uncertainties resulting from a significant underdamped piston mass, the effects of enclosed dead volume and leakage must be assessed.

3. Detailed Description of the Clearance-Sealed Piston Provers (DryCals)

The provers analyzed here consist of two modules[2]. A base unit contains the power supply, computer, keyboard and display. An interchangeable measuring cell contains the entire pneumatic and sensor systems.

Figure 2. DryCal ML-500

The Laboratory Master Provers are enhanced versions of the commercial DryCal ML-500, which is shown in Figure 2. Three ML-500 measuring cells have been extended from 5 inches to 8 inches and the measured flow paths increased to 5 inches (small cell) and 4 inches (medium and large cells). Presently, the three master cells cover the range of 10mL/min to 50 L/min. The target ML-500 cells, in turn, have ranges of 4 sccm to 50 slm.

[1] U.S. Patent No. 5,440,925

[2] U.S. Patent No. 5,456,107

Figure 2. DryCal ML-500

Each cell consists of a machined base containing the inlet and outlet fittings, bypass valve, temperature sensor and pressure tap. The bypass valve is of a self-relieving, low pressure, large area design. It latches in either the open or closed position to minimize introduction of heat into the flow stream. The pressure tap is located at the entrance to the measuring cylinder to maximize accuracy.

The base serves as a mounting for the vertical measuring cylinder/piston assembly, which uses a clearance-sealed piston to minimize friction. The cylinder is made of borosilicate glass and the piston is made of graphite. Both materials have a similar, very low coefficient of thermal expansion, allowing a precise fit to be achieved over a reasonable range of working temperatures. The effective cylinder diameter is neither the piston diameter nor the cylinder diameter: Rather, it is an intermediate value.

Detector slits are mounted directly to the cylinder's outer surface for maximum repeatability. A support structure is also attached to the base. It holds infrared light emitters and detectors, as well as the cell's electronic circuitry. Each cell contains all signal processing circuitry, A/D conversion and an EEROM for calibration data. In this way, complete calibration (with the exception of the computer's time base) can be performed on each cell individually.

A functional diagram of a DryCal piston prover is shown in Figure 3. Inlet gas ordinarily flows through the bypass valve to the outlet. When a reading is to begin, the bypass valve closes and the incoming gas displaces a piston that moves through a cylinder. After the piston has been allowed adequate time to accelerate, the time needed to pass from one optical sensor to another is measured. To the degree that the volume of the device is well known, we can derive the flow from measured primary dimensions (length and time).

Several additional elements of the practical design must also be considered. Temperature and absolute pressure sensors must be added to obtain standardized readings. The light detectors are collimated to increase accuracy. Finally, there is unavoidable dead volume consisting of the inlet fitting and tubing, interior passages, the valve and the portion of the cylinder below the point at which timing begins.

4.1 Measured Piston Diameter

The main precaution to be observed in measuring the piston diameter is to avoid deflection of the graphite piston by a measuring device. To avoid this problem, diameter is measured with a laser micrometer. Several readings are averaged to enhance accuracy.

4.2 Effective Piston diameter

This subject is analyzed in detail in our previous publication [1]. The following is a synopsis:

Direct measurement of the inside diameter of small cylinders over a relatively large distance is very difficult. For this reason, we use the instrument's internal self-test of the piston's leakage rate, the piston's weight and the viscosity of gas to calculate the maximum cylinder inner diameter using the Poiseuille-Couette equations.

The aspect ratio of the gap is over 1000:1, so we can safely assume the flow within the gap to be laminar. Therefore, we know the effective diameter to be that of the piston plus the gap (½ of the gap X 2).

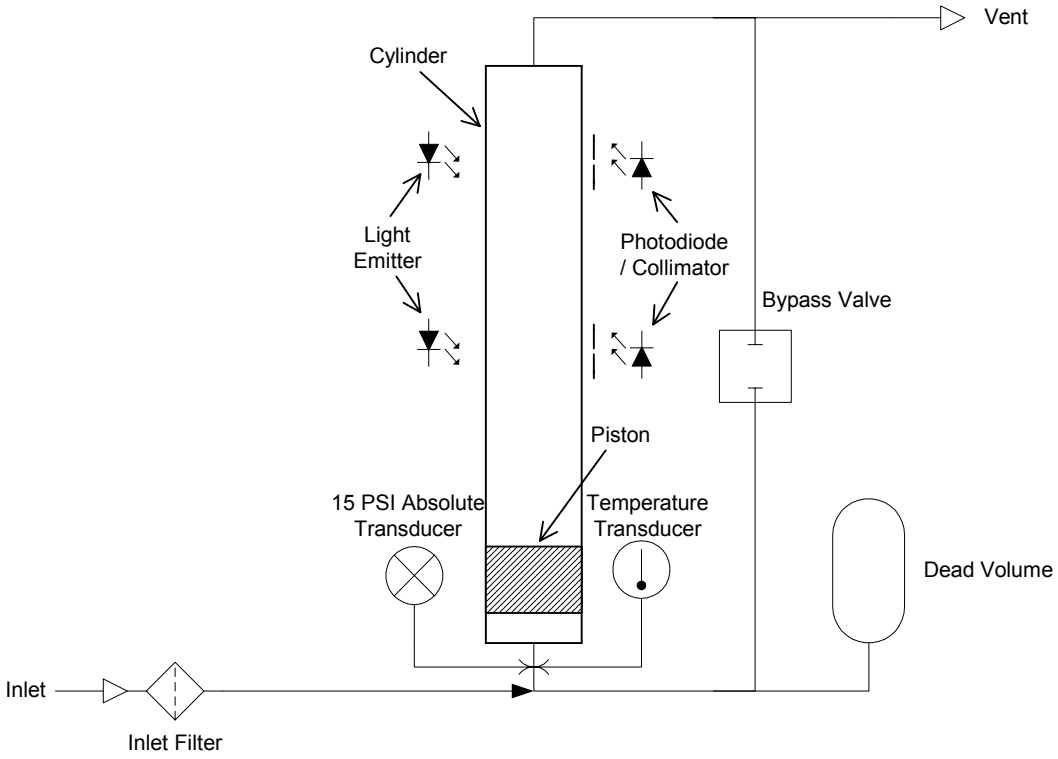

Figure 3 - Practical Piston Prover

However, we cannot state with absolute certainty what the effective piston diameter is. Experimental data shows that the piston touches the cylinder tangentially during leakage tests. We use that condition as our nominal case

We can conservatively estimate the maximum effective diameter to be that of an elliptical piston of such eccentricity that it touches the cylinder at two points, but which yields the same leakage as the nominal case. Taking a ratio of the two yields our maximum effective diameter. Because the eccentricities are so small, the results are equally valid for an eccentric cylinder.

With similar reasoning, we can find the effective diameter for a tapered cylinder. The limit case is a cylinder that touches the entire piston circumference at one end, with the piston touching tangentially at all other points. This yields our minimum case.

We calibrate the instrument to a diameter between the tapered limit case and the elliptical limit case. Then, for conservatism, we can assume a maximum error of half the difference between the two cases with a u-shaped probability distribution.

4.3 Measurement Length

The measurement length should be calibrated using the most representative method possible. The calibration is performed once the entire measuring cell is fabricated. The piston is positioned using a depth micrometer. The trip points actually detected by the mating optics and electronics are then used to determine the stroke length and its reproducibility.

4.4 Measurement Length Drift

Collimating slits attached to the glass cylinder's exterior mask the optical detectors. The effective width of the sensing slit is the actual slit width increased by the image of the emitter at the slit, reduced by any adaptive enhancement. The initial center-to-center spacing of the slits is a relatively straightforward measurement. However, significant potential uncertainty can arise from the position at which the sensor activates with respect to the slit. We must take into account the actual detector slit width, along with the size of the emitter's optical image at the detector slit (Figure 4).

The emitter is placed high enough to ensure that the light beam is always broken only by the edge of the piston furthest from the light source. This minimizes the geometric effect of the "optical lever" consisting of the distance from the piston edge to the sensor slit divided by the distance from the emitter to the piston edge. Specifically, $h_e = H_e\ (d_s/d_e)$. The effective detector slit width is then h_s+h_e.

Calibration based upon direct measurement of the distances at which the piston is detected can eliminate these uncertainties, but there is potential for significant drift from other sources:

- Light output of the emitters can change with age, temperature and voltage.
- Detector sensitivity can change with temperature and age.
- Ambient light levels can change.

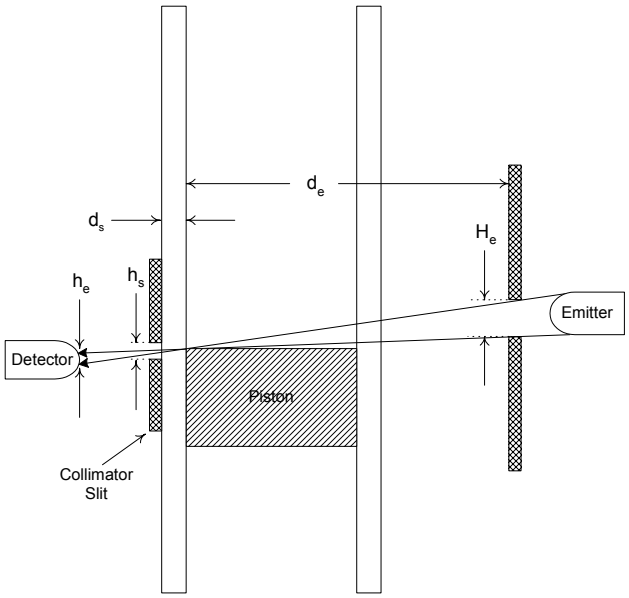

Figure 4 - Optical Geometry

To minimize drift, we use an adaptive measurement scheme. Before each cycle, a reading of the ambient light level is taken for each photodiode with the light emitters turned off. Then a reading is taken with the light emitters turned on. An average of the two levels is then set as the trip level for that cycle. This is shown in Figure 5.

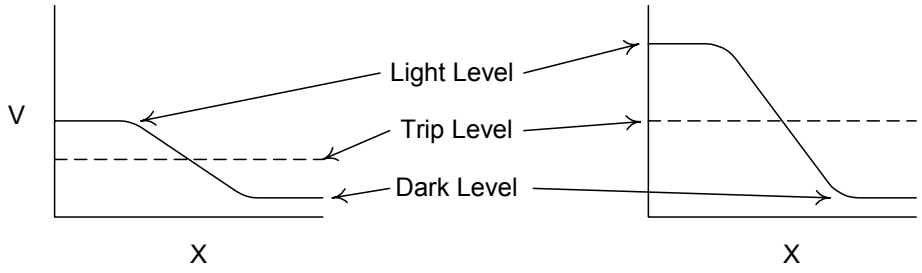

Figure 5 - Adaptive Detection

Using a fast A/D converter, we then measure the output of the photodiodes at intervals of approximately 150 microseconds during the piston's cycle of motion. We can reasonably assume that the geometry of the optical system does not change with time. Rather, the expected changes all affect the system's sensitivity. With a perfect A/D converter, we would then be able to eliminate all detector drift. For a practical converter, we will very conservatively assume a minimum signal level of 20 least significant bits (out of 4096 for our 12-bit converter). The effective detector slit width will then be the width calculated from the geometry previously described, reduced by a factor of 20:1.

4.5 Leakage

Leakage will limit the instrument's accuracy at very low flows. The instrument is tested for piston leakage by raising the piston to the topmost position, sealing the inlet and timing the passage of the piston from the upper sensor to the lower sensor. The instrument then calculates flow rate by dividing the subtended volume by the time.

Since we know the piston's weight, the measured leak rate is also used to calculate the effective cylinder diameter [1].

4.6 Dynamic Pressure Change

The DryCal is intrinsically a volumetric prover. As a piston prover is potentially subject to accelerative, oscillatory and piston-jamming effects, internal dynamic pressures must be measured to minimize uncertainty. To a first order, pressure only needs to be measured at the beginning and end of the timed measurement period. From the Ideal Gas Law, flow will be given by:

$$F = F_I \left[\frac{P_2}{P_A} + \left(\frac{P_2 - P_1}{P_A} \right) \frac{V_D}{V_M} \right]$$

Where:

F = Flow
F_I = Uncorrected Flow
P_A = Ambient Pressure
P_1 = Pressure at start of timed period
P_2 = Pressure at end of timed period
V_D = Dead Volume
V_M = Measured Volume

Uncorrected, the measured volume contains an error equal to the difference in internal pressure at the start and the end of the measuring period, amplified by the ratio of dead volume to measurement volume, as well as that of the pressure within the cylinder at the end of the timed period. The DryCal is a high-speed device. As a result, the internal pressure changes rapidly and can significantly affect measurement uncertainty.

For this reason, true dynamic pressure measurement has been incorporated in this prover. Once the dynamic pressure correction is determined, it is used to correct for the potential uncertainty, thereby enhancing the instrument's accuracy. With knowledge of the dead volume, which will be constant for a given instrument design using a specified amount of external dead volume, the uncertainty resulting from the dynamic pressure differences can be minimized. This approach's effectiveness is limited by the pressure measurement's total accuracy (including secondary uncertainties such as synchronicity and quantization) and the dead volume's accuracy.

4.7 Piston Rocking

The piston can rotate about its center until its diagonally opposed edges contact the cylinder walls, causing an uncertainty in the height of the measured edge with respect to the center. However, quantitative analysis shows that the maximum uncertainty for these closely fitted pistons is less than 2 ppm.

4.8 Thermal Expansion

The graphite piston and the borosilicate glass cylinder have similar thermal coefficients of expansion of approximately $7X10^{-6}$/deg C. Over the maximum laboratory temperature range, specified as ±3 degrees Celsius, the maximum dimensional variation will be 21 ppm. This variation will apply to diameter and stroke length, resulting in a sensitivity coefficient of 3.

4.9 Collection Time

4.9.1 Time Base Calibration

The time base consists of a crystal oscillator that clocks the MCU's free-running 16-bit counter. A frequency counter is used to verify the crystal's rated accuracy of ±0.005%. The counter is applied after buffering to prevent probe errors.

4.9.2 Timer Quantization

The photodetectors are adaptively measured every 150 microseconds. This process introduces a quantization error of ±75 microseconds. Since the measured time interval varies inversely with flow
($T = V / F$), the quantization error is largest for the highest flow.

4.9.3 Calculation and Display Quantization

Other quantization errors occur as a result of the display resolution and computer's internal divide subroutine. These errors are kept insignificant by designing to the proper degree of precision. The divide routine's resolution will be lowest at the highest flows, as it will be dividing a constant by a low time interval value.

5. Uncertainty Contributions - Laboratory Master Provers

It was not necessary to measure all of the uncertainty sources previously described. Many of them affect only repeatability. As these are automatic high-speed provers, it was simple to collect adequate statistical data to include them in Type A analysis.

5.1 Type A Uncertainties

5.1.1 Repeatability of Readings (Piston oscillations, rocking, detector trip point, quantization)

Each of the three sizes of provers was connected to a stable flow source. After temperature stabilization, 100 readings were taken and analyzed for their standard deviation (including readout quantization). The results are tabulated in Table 1. It should be noted that this is a very conservative evaluation, as laboratory temperature changes and flow source changes are included in the resulting uncertainties.

Table 1. Repeatability of Readings

Size	Flow (mL/min)	u	Maximum u
S	30	0.032%	0.032%
S	100	0.031%	
S	200	0.019%	
S	400	0.028%	
M	100	0.020%	
M	2000	0.027%	
M	4000	0.030%	0.030%
M	8000	0.026%	
L	10000	0.029%	
L	25000	0.034%	0.034%

5.1.2 Leakage

The reproducibility of leakage measurements was experimentally determined as described in Appendix I. The uncertainty was on the order of 14.9% of the leakage with a sensitivity of 1/3.

This has an effect of less than 5% of the effective piston diametric uncertainty, making it statistically insignificant for diameter determination.

The leakage is, of course, very significant in determining the lower flow limit of the cells. The leakage itself was 0.039, 0.11 and 0.31 mL/min for the three cells. If we correct by adding the measured leakage from the readings, we still must contend with the leakage's uncertainty. This is approximately 0.006, 0.016 and 0.046 mL/min for the three sizes. After the basic uncertainty analysis, we included the leakage uncertainty in a further, low-end analysis.

5.2 Type AB and B Uncertainties

5.2.1 Measured Piston Diameter

The average piston diameter was measured using a laser micrometer. An accredited laboratory measured three diameters at 120-degree intervals at distances of one third and two thirds of the piston's height from one edge. The six readings were averaged to obtain the piston diameter. The expanded uncertainty stated by the measuring laboratory was 40 microinches.

Assuming a coverage factor of two, the uncertainty of the readings is 0.51 microns. Dividing by the piston diameters, we obtain uncertainties of 55, 22 and 11 ppm for the small, medium and large provers respectively. Since the volume is affected by the square of the diameter, the sensitivity factor is 2.

5.2.2 Effective Piston Diameter

The effective piston diameter is the mean measured diameter plus one half of the annular gap as calculated in Appendix I. Its limit values are:

$$D = D_m + (0.685 \pm 0.160) \bullet \sqrt[3]{\frac{3F\mu h D_m}{wg}}$$

Where:
D = Effective piston diameter
D_m = Measured piston diameter
F = Leakage flow rate
μ = Viscosity of air
h = Piston height
w = Piston weight
g = 980.7 cm/sec^2

As the limit cases of taper and eccentricity cannot coexist, it is conservative to use a u-shaped distribution. Uncertainty is then:

$$u = \frac{0.160 \bullet \sqrt[3]{\frac{3F\mu h D_m}{wg}}}{D_m} \bullet \frac{1}{\sqrt{4.5}}$$

Effective piston diameter uncertainties are found in Table 2. Since the volume is affected by the square of the diameter, the sensitivity factor is 2.

Table 2. Effective Diametric Uncertainties

Size	Leakage (ml/min)	Diameter Correction	Variation (ppm)	u (ppm)
S	0.039	+0.049%	113	53
M	0.11	+0.023%	51	24
L	0.31	+0.016%	36	17

5.2.3 Measurement Length

The length of the timed stroke is determined by measuring the location optical detectors using a depth micrometer to move the piston. The location of each detector was measured separately. A number of readings were taken for each detector. Each reading reproduced the others within the digital micrometer's resolution of 0.0001 inches. Including the micrometer's rated accuracy and dividing by 1.732 for a rectangular distribution, we calculated the uncertainties of Table 3. The sensitivity factor is 1.

Table 3. Detector Location Uncertainties

Size	Detector	Tolerance (micro in.)	Distance (inches)	u (ppm)
S	Lower	31	5.00	6
S	Upper	56	5.00	11
M	Lower	36	4.00	9
M	Upper	56	4.00	14
L	Lower	36	4.00	9
L	Upper	56	4.00	14

5.2.4 Time Base

The time base is derived from a crystal rated at (and measured to) ±0.005%, or 50 ppm. Applying the appropriate factor for a rectangular distribution, u = 50/1.732 = 29 ppm with a sensitivity factor of 1.

5.2.5 Pressure Correction

In a volumetric device, correction of pressure to ambient is far less significant than in a standardized device. The uncertainty is that of the sensitive gauge pressure transducer when referred to the ambient pressure. In the small and medium sized cells, a full-scale pressure range of 2.5 cm water column is sufficient to measure the instrument's difference from ambient. For the large cell, 5 cm water column is necessary. Thus, the sensor system uncertainties are reduced by the ratio of full-scale pressure to ambient pressure, or approximately 0.0025 and 0.005 respectively. Over our limited laboratory temperature range of ±3 degrees Celsius, a simple silicon integrated transducer has a total uncertainty of less than 1%. The uncertainty of the absolute transducer is reduced by a similar ratio. Using a rectangular distribution, the combined

uncertainty is 22 ppm for the small and medium provers, and 45 ppm for the large prover. The sensitivity factor is 1.

5.2.6 Thermal Drift

The cylinder and piston have matched coefficients of thermal expansion of 7 X $10^{-6}/^{\circ}$C. Our laboratory temperature specification allows a tolerance of ±3 $^{\circ}$C. The resulting variation is ±21 ppm with a square distribution, so u = 12 ppm. Expansion is in three dimensions, so the sensitivity factor is 3.

5.2.7 Detector Drift

In addition to the measurement length uncertainty, we must also estimate the drift of measurement length with changes over time in sensor efficiency and emitter output. Although we are using an adaptive detection scheme, its efficiency is limited by quantization of the A/D converter. This, in turn, reduces the geometric uncertainty by a factor of ±½ bit divided by the number of bits difference between the light and dark levels, with a rectangular distribution. With our 4096 bit A/D converter, it is simple to assure that we have at least 20 bits of signal. This will reduce the geometric piston location uncertainty by a factor of 40:1, with a rectangular distribution. The individual uncertainty is multiplied by the square root of two to represent the two independent detectors. The resulting uncertainties are shown in Table 4.

Table 4. Sensor Drift Uncertainties

Size	Slit Image (inches)	Separation (inches)	Variation (ppm)	u Total (ppm)
S	0.00079	5.00	79	64
M	0.0074	4.00	93	76
L	0.0069	4.00	87	71

6. Uncertainty Contributions - ML-500 Provers

The ML-500 provers have the same intrinsic error sources as the Laboratory Master Provers previously described. However, since they are volumetrically calibrated by transfer from the master provers, the dimensional calibration need not be considered. Rather, the new error sources of transfer calibration bias error, and temperature and pressure correction errors need to be assessed. In addition, some of the same error sources that appear in the laboratory provers' analysis also must be applied to the ML-500 devices. Following is a discussion of the ML-500 provers' uncertainties.

6.1 Type A Uncertainties

6.1.1 Repeatability

Since repeatability was the major error source for the laboratory provers, extensive data was collected for Type A analysis of the ML-500 provers. We tested several of each size cell, taking 100 readings at each of 5 flows logarithmically spaced throughout the cells' ranges. We then

calculated the standard deviation of each flow rate's 100 readings for each measurement point. Again, for conservatism, no attempt was made to remove flow generator and room temperature effects from the data.

We averaged the readings for each flow point for each cell. The results are presented in Table 5.

Table 5 – ML-500 Prover Repeatability

Small		Medium		Large	
Flow	U (ppm)	Flow	U (ppm)	Flow	U (ppm)
4	650	50	730	250	710
11	830	190	470	1000	350
42	520	690	450	3500	290
160	760	2600	470	13300	390
500	730	9000	470	50000	980
600	470				
800	470				

6.1.2 Calibration Transfer Error

To minimize transfer error, the ML-500 is placed adjacent to the Laboratory Master Prover and allowed to stabilize for two hours. The laboratory has an air circulation fan arranged to cause air to flow down the center of the laboratory, across the rear wall and then along the bench tops to minimize bench temperature gradients.

Using a precision flow source as a short-term transfer standard, readings are taken on a Laboratory Master Prover before and after reading the ML-500 under test. To statistically assess the transfer error, five averaged readings over the entire flow range from three ML-500s were normalized to their respective averages. The standard deviation of the fifteen readings so obtained, 646 ppm, was attributed to the laboratory and flow conditions that would cause transfer error. This uncertainty is equivalent to a temperature uncertainty of 0.20K, or a temperature range of ±0.35K. This is probably an excessive value, as temperature matching precautions and instrument similarities should have kept temperature differences to a much smaller value, and our flow generator instability is an order of magnitude smaller. Again, though, we retained the raw value to remain conservative.

6.1.3 Leakage

All ML-500 cells are calibrated for leakage and the average leakage value is added to each reading as a tare value. Statistical tests of leakage repeatability exhibited a standard deviation of 14.9 percent. Therefore, 14.9 percent of the leakage value divided by the flow is used as a flow-dependent uncertainty. For the small, medium and large cells, these uncertainties are 0.0075, 0.015 and 0.15 ccm.

6.2 Type AB and B Uncertainties

6.2.1 Pressure Correction

We measure pressure through a tap located just below the measuring cylinder for maximum correlation to cylinder pressure. We took care to avoid velocity effects that would alter pressure accuracy. We used a high-speed silicon transducer to allow dynamic correction as previously discussed.

We rate the calibrator for use at 22.5°C ± 7°C. The transducer was specified by its manufacturer over a larger temperature range. We treated the transducer linearity, zero and span errors as the

manufacturer's values proportioned by our temperature span divided by that of the manufacturer. We further divided the values by 0.9 to represent our use of less than full-scale output. The resulting uncertainty is shown in Table 6.

Table 6 – Pressure Transducer Uncertainty

Source	Value (ppm)	Distribution	Factor	u
Transducer Linearity	222	Rectangular	1.732	128
Transducer Zero Drift	1111	Rectangular	1.732	642
Transducer Span Drift	1111	Rectangular	1.732	642
A/D Quantization	658	Rectangular	1.732	380
Amplifier Drift	700	Rectangular	1.732	404
Calibration Error	1000	Rectangular	1.732	577
Net Pressure Uncertainty				1217

6.2.2 Temperature Correction

Temperature is measured by a well-insulated transducer located on the centerline of the gas stream just below the measuring cylinder. Again, the manufacturer's specifications were adjusted for our specified temperature range. The results are contained in Table 7.

Table 7 – Temperature Transducer Uncertainty

Source	Value (ppm)	Distribution	Factor	u
Transducer Linearity	676	Rectangular	1.732	391
A/D Quantization	671	Rectangular	1.732	387
Calibration Error	850	Rectangular	1.732	488
Reference Drift	350	Rectangular	1.732	202
Net Temperature Uncertainty				763

6.2.3 Drift

There are two dominant drift mechanisms. They are similar to those of the Laboratory Master Provers: Detector drift and thermal expansion.

6.2.3.1 Detector Drift

We use the same adaptive process discussed for the Laboratory Master Provers in the ML-500. However, the emitter images and slit heights are larger, and the measurement path is smaller. Table 8 presents the results after correction for rectangular distribution and for the error of two slits.

Table 8. ML-500 Detector Drift Uncertainties

Size	Slit Image (inches)	Separation (inches)	Variation (ppm)	u Total (ppm)
S	0.013	2.4	263	214
M	0.014	2.0	338	276
L	0.0013	1.5	420	343

6.2.3.1 Thermal Expansion

The measuring cylinder has a coefficient of thermal expansion of 7 ppm/K. Over our temperature range of 7K, allowing for three degrees of freedom and for a rectangular distribution, we have a resulting uncertainty of 85 ppm.

7. Uncertainty Statements

Following are separate uncertainty statements for the Laboratory Master Provers and the ML-500 ML-500 provers

7.1 Laboratory Master Provers

We base our uncertainty statement on the worst observed (Type A) reproducibility error for each cell size. Table 9 gives the maximum uncertainty for all but the lowest flows.

At the minimum flows, leakage uncertainty must be included. The expanded uncertainty remains below 0.1% for flows above 10, 25 and 80 mL/min for the three cells.

Table 9. Laboratory Master Uncertainty Statement

	Type	Small u (PPM)	Med u (PPM)	Large u (PPM)	Sens. Factor	Small Net u (PPM)	Med Net u (PPM)	Large Net u (PPM)
Reproducibility (99 d/f)	A	300	320	340	1	320	300	340
Measured Piston Diameter	B	55	21	11	2	110	42	22
Effective Piston Diameter	B	53	22	17	2	107	44	34
Upper Detector Location	B	6	9	9	1	6	9	9
Lower Detector Location	B	11	14	14	1	11	14	14
Time Base	B	29	29	29	1	29	29	29
Pressure Correction	B	22	22	44	1	22	22	44
Thermal Expansion	B	12	12	12	3	36	36	36
Detector Drift	B	64	76	71	1	64	76	71
Total u (percent)						0.036%	0.032%	0.036%
Coverage Factor						2	2	2
Overall Uncertainty (percent)						0.073%	0.064%	0.071%

7.2 ML-500 Provers

Since we wish to characterize the ML-500 over its range, we will first calculate the flow-independent uncertainty and then calculate the total uncertainty over a range of tested flows for each cell size.

7.2.1 Flow-Independent Uncertainty

The flow-independent sources are summarized in Table 10.

Table 10 – Flow-independent Uncertainties

Source	Type	Small u (PPM)	Medium u (PPM)	Large u (PPM)
Master Prover	AB	365	320	355
Calibration Transfer	A	646	646	646
Pressure Correction	B	1217	1217	1217
Temperature Correction	B	763	763	763
Detector Drift	B	214	276	343
Thermal Expansion	B	85	85	85
Combined Flow-Independent		1633	1633	1652

7.2.2 Total Uncertainty

Finally, we can combine the flow-independent uncertainties of Table 10 with the flow-dependent uncertainties of Table 5 and the leakage uncertainties of 6.1.3 to obtain the expanded uncertainties of Table 11.

Table 11 – ML-500 Prover Expanded Uncertainty (2X)

Small		Medium		Large	
Flow	U	Flow	U	Flow	U
4	0.524%	10	0.467%	60	0.616%
11	0.391%	25	0.377%	120	0.438%
42	0.345%	50	0.363%	250	0.379%
160	0.360%	190	0.340%	1000	0.339%
500	0.358%	690	0.339%	3500	0.336%
600	0.340%	2600	0.340%	13300	0.340%
800	0.340%	9000	0.340%	50000	0.384%

The data of Table 11 can be visualized more easily in graphical form, as shown in Figures 6-8. We have added a “worst case” line to each, representing cells that exhibit 5/3 of the previously observed repeatability errors, the maximum that we expect to ever see in future production.

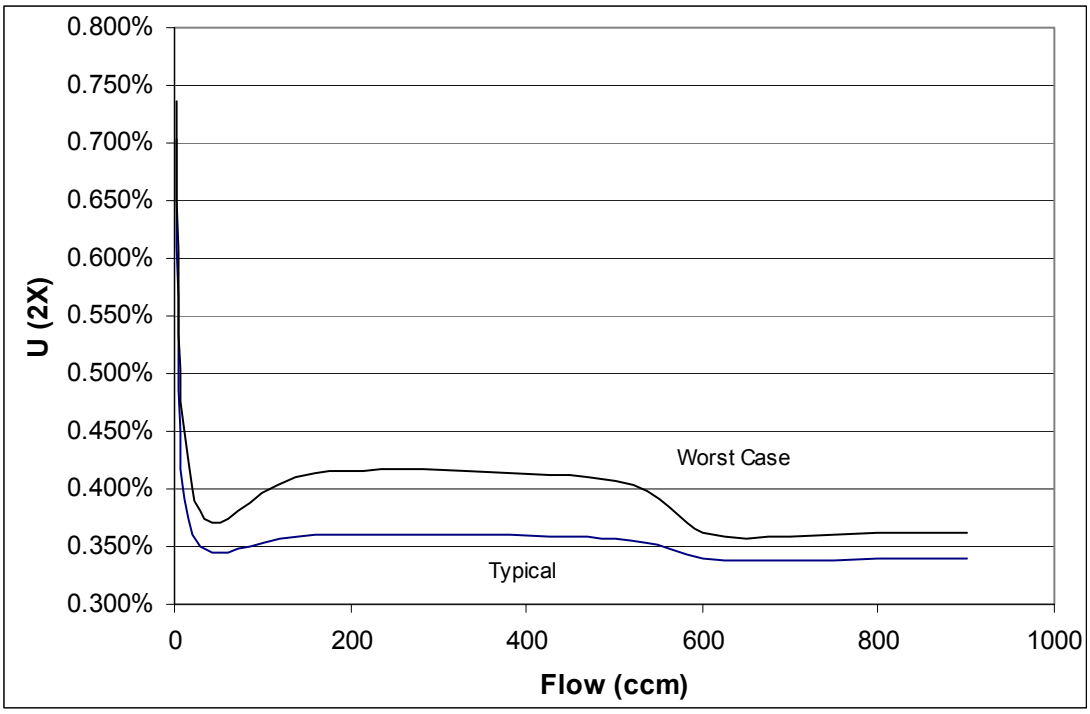

Figure 6 – ML-500 Low Flow Cell Expanded Uncertainty (2X)

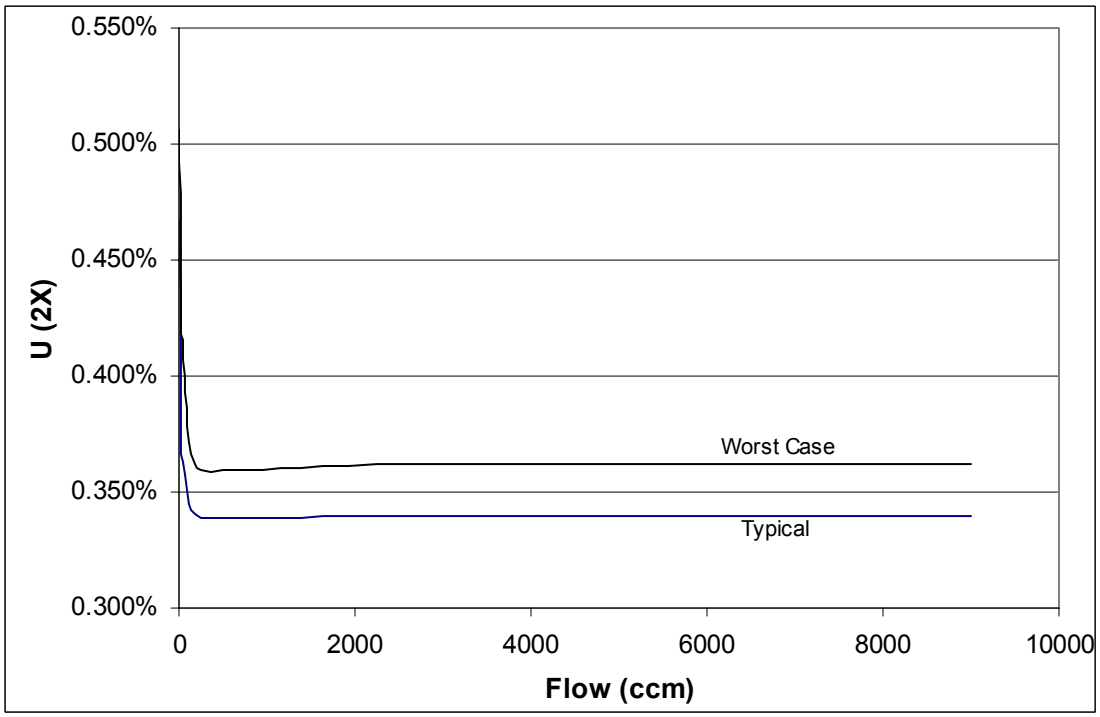

Figure 7 – ML-500 Medium Flow Cell Expanded Uncertainty (2X)

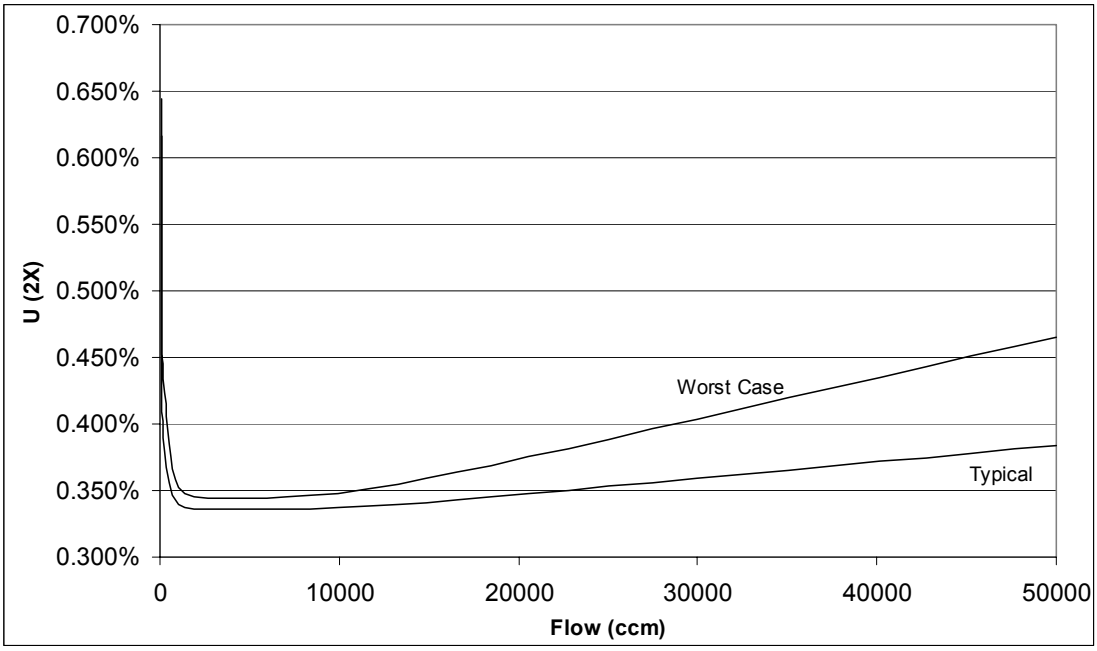

Figure 8 – ML-500 High Flow Cell Expanded Uncertainty (2X)

8. Conclusions

This analysis shows that the ML-500 easily meets our original design goal of 0.5% expanded uncertainty over turn down ranges of hundreds to one. In fact, the range of 5 sccm to 50000 sccm could be covered by two of the three cells (albeit using increased measurement times). Alternatively, uncertainties on the order of 0.35% to 0.4% can be obtained over most of the range.

We also note that we can extend the laboratory master standards into commercial products in the 0.2% to 0.25% range, but much lower uncertainties must first be achieved for the pressure and temperature sensors.

Reference:

1. H. Padden, Uncertainty Analysis of a High-Speed Dry Piston Flow Prover, *Measurement Science Conference*, Anaheim, CA, 2002 (contact author at padh@biosint.com for reprints)